Proceedings Paper:
Lampert, Thomas and O'Keefe, Simon (2008) Active Contour Detection of Linear Patterns in Spectrogram Images. In: 19TH INTERNATIONAL CONFERENCE ON PATTERN RECOGNITION, VOLS 1-6. 19th International Conference on Pattern Recognition (ICPR 2008), 08-11 Dec 2008 IEEE, Tampa, pp. 3350-3353.

https://doi.org/10.1109/ICPR.2008.4761214

Active Contour Detection of Linear Patterns in Spectrogram Images

Thomas A. Lampert
The University of York, UK
tomal@cs.york.ac.uk

Simon E. M. O'Keefe
The University of York, UK
sok@cs.york.ac.uk

Abstract

This paper proposes an extension to the active contour algorithm for the detection of linear patterns within remote sensing and vibration data. The proposed technique uses an alternative energy force, overcoming the limitations of the original algorithm, which relies upon simple energy formulations to extract intensity and gradient information from an image. We overcome these by forming a noise model, which is used to detect a feature's presence, and by integrating information from several locations within an image to strengthen the detection process.

1. Introduction

The active contour model proposed by Kass et al. [7] allows for non-parametric feature detection within an image. The active contour is constrained by internal energy forces, which ensure that the active contour's shape follows certain criteria; these are typically defined as curvature and connectivity. It is guided by an external energy force which attracts the active contour towards features by following local changes in energy gradient. As these gradients are calculated on a local basis the active contour needs to be initialised close to the desired feature to ensure a correct convergence. To overcome this Cohen [3] proposes a force which expands a closed active contour until it reaches the boundary from any initial position within it, called the balloon force. Alternatively points of the boundary may be selected prior to the contour's evolution [4]. The active contour converges on a minimum of the weighted combination of its internal and external energy constraints which, subject to the internal constraints, translates to a local gradient maximum in the image. The active contour thus detects features which are distinguishable by gradient. This technique has proved valuable in the area of medical imaging, specifically; cortex [5] and calcaneus boundary detection [8] and brain segmentation [9].

The original algorithm has a single contour, is dependent on gradient features and is sensitive to the initial location. Here we present an active contour model for the detection of features in remote sensing and vibration data. For this application we derive a novel external energy constraint which allows the model to detect very weak structures not defined by gradient and introduce an additional energy term which overcomes the initialisation problem.

This paper is laid out as follows: in Section 2 the original active contour algorithm is outlined and our novel contributions are defined. In Section 3 experimental results are presented and discussed. Finally, in Section 4, our conclusions are drawn.

2. Method

2.1. The Active Contour Algorithm

The original active contour model, as proposed by Kass et al. [7], is as follows. A set of snake points, $\boldsymbol{v}(s) = (x(s),\ y(s))$, $s = 0, 1, \ldots, n-1$, forms a deformable contour where $x(s)$ and $y(s)$ are the contour point's position in the image such that $x(s) \in [0, x_{max}]$ and $y(s) \in [0, y_{max}]$. The contour has the energy

$$\mathcal{E}(\boldsymbol{v}) = \int_0^1 \alpha \left| \frac{\delta \boldsymbol{v}(s)}{\delta s} \right|^2 + \beta \left| \frac{\delta^2 \boldsymbol{v}(s)}{\delta s^2} \right|^2 + \mathcal{P}(\boldsymbol{v}(s)))ds \tag{1}$$

where the terms α and β control the continuity and curvature of the contour (respectively) and the term $\mathcal{P}$ corresponds to the external energy derived from the image.

The external energy force, $\mathcal{P}$, attracts the contours to edges in the image. In the original algorithm these are taken to be the image intensity or gradient (2).

$$\mathcal{P}(\boldsymbol{v}(s)) = -|\nabla I(\boldsymbol{v}(s))|^2 \tag{2}$$

2.2. Active Contour for Pattern Detection

For the detection of features in the proposed domain there are two issues limiting the active contour's appli-

978-1-4244-2175-6/08/$25.00 ©2008 IEEE

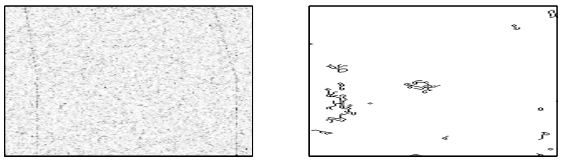

(a) (b)

Figure 1. (a) A low SNR image. (b) Canny edge detection.

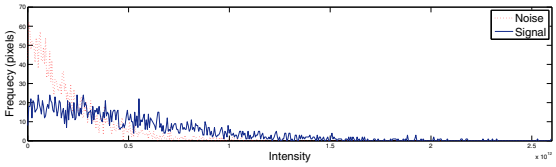

Figure 2. Histogram of pixel intensity values for the signal and noise classes in a 3dB SNR image.

cation: its sensitivity to initialisation and the assumption that features are defined by gradient.

2.2.1. Initialisation. To overcome the initialisation problem, a similar force to Cohen's balloon force is used. We define an external force which 'walks' the contour in a horizontal direction across the x-axis. The force is given by

$$\mathcal{W}(\boldsymbol{v}(s)) = -x(s)c \tag{3}$$

where c is a constant which is balanced to overcome noise introduced by the external energy while not forcing the contour to miss true detections. The contour will encounter vertical features during its walk.

2.2.2. External Energy Force. In this application, gradient and image intensity information are not sufficient to define features. As illustrated in Fig. 1, in very noisy images which contain weak features, using the Canny [2] filter produces spurious edge detections and fails to detect features. It can also be seen in a histogram of intensity values for a 3dB SNR image, Fig. 2, that the noise and signal classes overlap considerably. We form an energy term which is based upon pixel intensity values contained within a window $\boldsymbol{W}(x, y)$ (and therefore incorporating spatial information). The window vector is then projected onto basis vectors derived through Principal Component Analysis (PCA) to remove noise and to reduce the dimensionality (avoiding the 'curse of dimensionality' [1]) of the data. We create a noise model by fitting a Gaussian distribution to examples of noise which is used to form a measure of windows' content. This measure is formulated to take a maximum value when the window contains a pattern section and a minimum value otherwise.

The feature vector $\boldsymbol{x}$ is defined as a linear arrangement of pixel values from a window $\boldsymbol{W}(x, y)$ centred on pixel (x, y) of the image I. n is the height and m the width of the window. A training set $\boldsymbol{X}$ of nm columns is formed which includes an equal number of examples from windows containing a feature and those containing only noise. The principal component vectors $\boldsymbol{u}_k$, are found by maximising the quantity λ_k as follows

$$\lambda_k = \frac{1}{n}\sum_{i=1}^{n}(\boldsymbol{u}_k^T(\boldsymbol{x}_i - \bar{\boldsymbol{x}}))^2$$

where $\bar{\boldsymbol{x}}$ is the mean vector of $\boldsymbol{X}$, subject to the orthogonality constraint

$$\boldsymbol{u}_l^T\boldsymbol{U}_k = \delta_{lk}$$

A subset, $\boldsymbol{U}$, is selected as the first d principal components and the training data projected onto them to form $\hat{\boldsymbol{X}}$.

$$\boldsymbol{U} = [\boldsymbol{u}_1, \ldots, \boldsymbol{u}_d] \tag{4}$$
$$\hat{\boldsymbol{X}} = \boldsymbol{U}^T\boldsymbol{X}$$

By storing $\boldsymbol{U}$, window vectors derived as the active contour evolves can be projected into the same PCA space. A plot of a data set $\hat{\boldsymbol{X}}$ containing noise and signal examples with a SNR of 3, 6 and 9dB projected onto the first 2 principal components can be seen in Fig. 3. It shows that this method results in clear separation of the noise and signal classes and a representation in which the noise can be easily modelled using a Gaussian distribution. Also, an increase in SNR translates to increased distance from the noise class. The three pronged fan structure that is observed results from windowing.

The parameters for a multivariate Gaussian distribution, $\boldsymbol{\mu}$ and $\boldsymbol{\Sigma}$, are selected to fit the noise examples present in $\hat{\boldsymbol{X}}$.

$$\boldsymbol{G}(\boldsymbol{v}(s)) = \frac{1}{(2\pi)^{\frac{d}{2}}|\boldsymbol{\Sigma}|^{\frac{1}{2}}}exp^{[-\frac{1}{2}(Q)^T\boldsymbol{\Sigma}^{-1}(Q)]} \tag{5}$$

$$Q = \boldsymbol{U}^T\boldsymbol{W}(\boldsymbol{v}(s)) - \boldsymbol{\mu}$$

where $\boldsymbol{U}^T$ are the principal components derived in (4), $\boldsymbol{W}(\boldsymbol{v}(s))$ is the vector of pixel values from a window centred on contour point $\boldsymbol{v}(s)$ and $\boldsymbol{\mu}$ and $\boldsymbol{\Sigma}$ are the mean and standard deviation of the PCA projected noise vectors. A subset of $\hat{\boldsymbol{X}}$ which contains only noise vectors

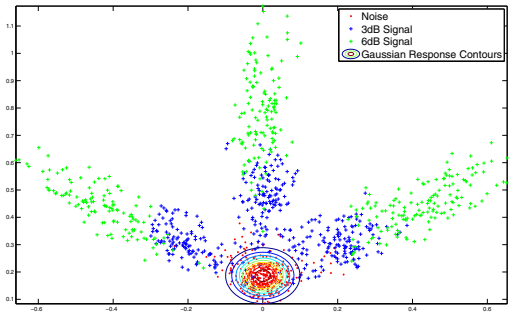

Figure 3. Windowed feature vectors projected onto 2 principal components (window size: 21 x 3 pixels).

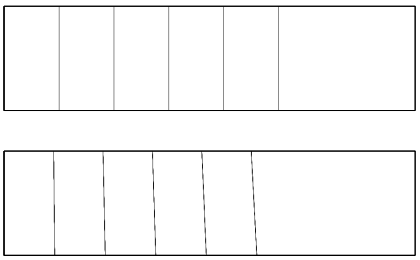

Figure 4. Ground truth image templates for a straight pattern section (top) and a sloped pattern section (bottom).

will be defined as $\hat{\boldsymbol{X}}^n \subset \hat{\boldsymbol{X}}$, therefore $\boldsymbol{\mu}$ and $\boldsymbol{\Sigma}$ can be calculated using the maximum likelihood estimators [6]

$$\boldsymbol{\mu} = \frac{1}{n}\sum_{i=1}^{n} \hat{\boldsymbol{x}}_i^n \tag{6}$$

$$\boldsymbol{\Sigma} = \frac{1}{n}\sum_{i=1}^{n} (\hat{\boldsymbol{x}}_i^n - \boldsymbol{\mu})(\hat{\boldsymbol{x}}_i^n - \boldsymbol{\mu})^T \tag{7}$$

where $\forall \hat{\boldsymbol{x}}^n \in \hat{\boldsymbol{X}}^n$ is a vector containing noise. The contours of a 2D Gaussian distribution fitted to the noise class are shown in Fig. 3.

We use a single Gaussian distribution to model the noise and anything at the distribution's extreme is classified as signal. This is useful as the characteristics of the feature can vary greatly but the noise is consistent.

Now $\mathcal{P}$ in eq. (1) can be rewritten to use the Gaussian's response to a novel window as an external energy force.

$$p(\boldsymbol{v}(s)) = \begin{cases} 1 & \text{if } \boldsymbol{G}(\boldsymbol{v}(s)) \geq t \\ \boldsymbol{G}(\boldsymbol{v}(s)) & \text{if } \boldsymbol{G}(\boldsymbol{v}(s)) < t \end{cases}$$

The purpose of the threshold t is to smooth the background noise in the active contour's search space; thus simplifying the detection problem.

Incorporating *a priori* information regarding a pattern set P_s (composed of relative positions of a pattern), can improve detection rates and form a pattern-based active contour search. As track patterns can be related through some underlying relationship, window samples, and their Gaussian response, can be taken from locations relative to the contour point's position in the x-axis (for vertical lines) as defined in a pattern set P_s.

$$\begin{aligned} \mathcal{P}(\boldsymbol{v}(s)) &= \mathcal{W}(\boldsymbol{v}(s)) + \frac{\gamma}{N+1}(p(\boldsymbol{v}(s)) \\ &\quad + \sum_{n=1}^{N} p(fq_n x(s), y(s))) \end{aligned} \tag{8}$$

Where $\mathcal{W}(\boldsymbol{v}(s))$ is the walk force (3), $p(\boldsymbol{v}(s))$ is the external energy calculated at the true contour position, $p(fq_n x(s), y(s))$ is the external energy calculated at the nth relative position $\forall fq_n \in Ps$ and N is the cardinality of the pattern set P_s. Averaging over a pattern set results in the flattening of noise spikes and the reduction of responses from all but the first feature in the pattern set; reducing the risk of multiple detections of a pattern.

We are looking for vertical, curvilinear features, so the first and last points of the contour are fixed to the top and bottom of the image such that $\boldsymbol{v}(0) = [x(s), v]$ and $\boldsymbol{v}(n-1) = [x(s), y_{max} - v]$. Movement of contour points will be restricted to the x-axis to ensure that an even search takes place in this direction. Using the proposed energy term and model the contour can now be thought of as a 'mesh' which stretches across the image, similar to a flexible correlation template.

3. Experimental Results

The experiments outlined in this section use images containing the same linear pattern set ($P_s = \{2, 3, 4, 5\}$) with SNRs ranging from 0 to 10dB. Ground truth templates for the images are shown in Fig. 4.

3.1. Parameter Selection

To enable the contour to perform its detection using the maximum amount of information derived from the

image the external energy weight, γ, is set to $\gamma = 1$. The internal energy parameters α and β are set to $\alpha = 0.1$ and $\beta = 0.2$ to allow the contour sufficient freedom to model variations within the pattern.

A training set containing 1000 examples of noise and 1000 examples of 0dB mean SNR signal and noise was formed from 21 x 3 pixel windows. In this way the principal components represent the direction of maximum variance for windows containing 0dB tracks and therefore SNRs greater than 0dB will be better separated from the noise. It was found through eigenvalue analysis that 2 principal components capture the majority of the data's variance. The parameters t and c are set to $t = 0.00008$ and $c = 0.41$; values determined through experimentation. A model for determining these parameters will be published in future work.

3.2. Results

The proposed algorithm correctly detects $> 92\%$ of straight line patterns in images containing a mean SNR of 1.5dB or above, see Fig. 5 (top). It can also be seen that below a mean SNR of 1.5dB the detection process gradually degrades until at a mean SNR of 0dB none of the pattern is detected. This clearly indicates that the class distributions, as used by the external energy term, become less distinguished at lower SNRs. Sloped patterns are detected at a rate of $> 90\%$ up until the mean SNR is reduced to 3dB, at which point the performance reduces in a roughly linear fashion to 0% at 0.5dB. It can be expected that sloped patterns are not detected as reliably as straight patterns because, currently, the external energy is specifically trained using vertical, straight, patterns.

It can be observed that the presented algorithm provides very good localisation results; at all SNRs, when a pattern is detected it is, on average, within 1 pixel of the true location, see Fig. 5 (bottom). It should also be mentioned that given that the noise is correctly modelled during the training process no false positives are detected.

4. Conclusion

We have presented an active contour framework, including a novel external energy term, with application to remote sensing and vibration data. The contributions of our model are: its use of *a priori* information regarding pattern structure to enhance detection, the novel external energy term and its ability to detect structure which can vary greatly. As the results indicate, combining these contributions allows for structure detection at low SNRs.

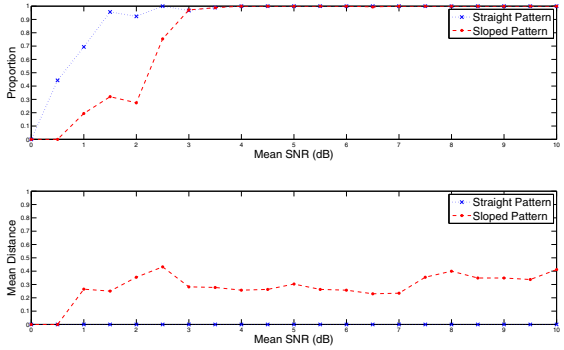

Figure 5. Proportion of patterns detected with less than 5 pixels difference at varying levels of mean SNR (top). Mean distance from the true location of the detected patterns (bottom).

Acknowledgements

This research has been supported by QinetiQ Ltd. with special thanks to Jim Nicholson for guiding the objectives and providing the synthetic data.

References

[1] C. M. Bishop. *Neural Networks for Pattern Recognition*. Oxford University Press Inc., 1995.

[2] J. F. Canny. A computational approach to edge detection. *IEEE Trans. on Pattern Anal. and Mach. Intell.*, 8(6):679–698, November 1986.

[3] L. D. Cohen. On active contour models and balloons. *Computer Vision, Graphics, and Image Processing. Image Understanding*, 53(2):211–218, 1991.

[4] L. D. Cohen and R. Kimmel. Global minimum for active contour models: A minimal path approach. *Int. J. of Computer Vision*, 24(1):57–78, 1997.

[5] C. Davatzikos and J. Prince. An active contour model for mapping the cortex. *IEEE Trans. on Medical Imaging*, 14(1):65–80, 1995.

[6] R. O. Duda, P. E. Hart, and D. G. Stork. *Pattern Classification*. Wiley-Interscience Publication, 2000.

[7] M. Kass, A. Witkin, and D. Terzopoulos. Snakes: Active contour models. *Int. J. of Computer Vision*, 1(4):321–331, 1988.

[8] F. Lefebvre, G. Berger, and P. Laugier. Automatic detection of the boundary of the calcaneus from ultrasound parametric images using an active contour model: Clinical assessment. *Medical Imaging*, 17(1):45–52, February 1998.

[9] H. Li, A. Yezzi, and L. D. Cohen. 3D brain segmentation using dual-front active contours with optional user interaction. *Int. J. of Biomedical Imaging*, 2006:Article ID 53186, 17 pages, 2006.